1 **Data driven prioritization and review of targets for molecular based**

2 **theranostic approaches in pancreatic cancer**

3

4 **Authors:** Marjory Koller[1*], Elmire Hartmans[2*,] Derk Jan A de Groot[3], Xiao Juan Zhao[3],

5 Gooitzen M van Dam[4], Wouter B Nagengast[2*†], Rudolf S N Fehrmann[3*†]

6 *Contributed equally; †Corresponding authors

7

8 **Affiliations:**

9 1. Department of Surgery, University of Groningen, University Medical Centre Groningen, Groningen, the

10 Netherlands;

11 2. Department of Gastroenterology and Hepatology, University of Groningen, University Medical Centre

12 Groningen, Groningen, the Netherlands;

13 3. Department of Medical Oncology, University of Groningen, University Medical Centre Groningen,

14 Groningen, the Netherlands;

15 4. Department of Surgery, Nuclear Medicine and Molecular Imaging and Intensive Care, University of

16 Groningen, University Medical Centre Groningen, Groningen, the Netherlands;

17

18 **Corresponding author:** Wouter B Nagengast[2] and Rudolf S N Fehrmann[3], University Medical Centre

19 Groningen (UMCG), Hanzeplein 1, PO-box 30 001, 9700 RB Groningen, The Netherlands, phone number:

20 +3150 3612620 / Fax number: +3150 3619306, w.b.nagengast@umcg.nl / r.s.n.fehrmann@umcg.nl

21

22 **Word count: 4000**

23

24 Running title: *Theranostic targets in pancreatic cancer*

25

26

27   **ABSTRACT**

28   Molecular targeted therapeutical and imaging strategies directed at aberrant signaling-

29   pathways in pancreatic tumor cells may improve the poor outcome of pancreatic ductal

30   adenocarcinoma (PDA). Therefore, relevant molecular targets need to be identified.

31   **Methods:** We collected publicly available expression profiles of patient derived normal

32   pancreatic tissue (n=77) and PDA samples (n=103). Functional Genomic mRNA

33   (FGmRNA) profiling was applied to predict target upregulation on the protein level. We

34   prioritized these targets based on current status of (pre)-clinical therapeutical and

35   imaging evaluation in PDA.

36   **Results:** We identified 213 significantly upregulated proteins in PDA compared to

37   normal pancreatic tissue. We prioritized mucin-1 (MUC1), mesothelin (MSLN), gamma-

38   glutamyltransferase 5 (GGT5) and cathepsin-E (CTSE) as the most interesting targets,

39   since studies already demonstrated their potential for both therapeutic and imaging

40   strategies in literature.

41   **Conclusion:** This study can facilitate clinicians and drug developers in deciding which

42   theranostic targets should be taken for further clinical evaluation in PDA.

43

44   **Keywords:** Pancreatic ductal adenocarcinoma (PDA), pancreatic cancer, theranostic

45   approach, targeted molecular therapy, targeted molecular imaging, genetic profiling,

46   biomarker

47

48

INTRODUCTION

PDA is the fourth leading cause of cancer-related mortality worldwide(1). Despite extensive surgery and improved chemotherapeutic regimens, the prognosis of PDA remains poor. Since symptoms often occur late in the disease process, the majority of patients present with locally advanced or even metastatic disease, resulting in a 5 years overall survival rate of only ~8% (*1*). Solely patients with local disease are candidate for curative surgical treatment. Despite the curative intent, the 5 years survival in the surgical treated patients is still as low as 20% (*2*). This poor survival is partially caused by the rapid development of metastases shortly after surgery. Most likely, this is due to microscopic dissemination that was already present at the time of surgery. Once distant metastases are present, the best available palliative chemotherapy regimen with the best overall survival rate is a combination of fluorouracil, leucovorin, irinotecan and oxaliplatin. However, the overall survival benefit is modest and the toxicity is significant (*3*).

In contrast to the traditional working mechanism of chemotherapy, which has a cytotoxic effect on all rapidly dividing cells, molecular targeted therapies more selectively target aberrant cell signaling-pathways that drive tumor growth. Therefore, in general molecular targeted therapies are expected to be more tumor specific, which could enhance therapy efficacy and decrease side-effects. However, patients that are likely to benefit from a particular targeted therapy have to be selected carefully, and target overexpression needs to be demonstrated. To date, target expression is determined by immunohistochemistry on tissue biopsies which are prone to be biased by sampling error due to heterogeneity of tumors and metastases. Theranostics which integrate diagnostics and therapeutics by fluorescently or radioactively labelling of drugs, can

73   provide insight in pharmacokinetics, tumor uptake and bio distribution of drugs which

74   might be used for clinical decision making and individualized management of disease.

75   To enable a theranostic approach in PDA patients, there is an unmet need for

76   identification and prioritization of relevant targets. To this end, we used the recently

77   developed method of FGmRNA-profiling to predict overexpression of target antigens on

78   the protein level (*4*). FGmRNA-profiling is capable to correct a gene expression profile of

79   an individual tumor for physiological and experimental factors, which are considered not

80   to be relevant for the observed tumor phenotype and characteristics.

81   The aim of this study was to identify potential target antigens in PDA using

82   FGmRNA-profiling that will facilitate clinicians and drug developers in deciding which

83   theranostic targets should be taken for further evaluation in PDA. Subsequently, an

84   extensive literature search was performed to prioritize these potential target antigens for

85   their utilization in a theranostic approach in the near-future.

86

87   **MATERIALS AND METHODS**

88   **FGmRNA-profiling: Identification of Upregulated Genes in PDA**

89   *Data acquisition*. We collected publicly available raw microarray expression data from

90   the Gene Expression Omnibus for the affymetrix HG-U133 plus 2.0 and the HG-U133A

91   platforms (*5*). We used automatic filtering on relevant keywords with subsequent manual

92   curation to include patient derived PDA samples and normal pancreatic tissue. Cell line

93   sample were deemed irrelevant and excluded for further analysis.

94   *Sample processing*. Non-corrupted raw data files were downloaded from the Gene

95   Expression Omnibus for the selected samples. After removal of duplicate files, pre-

96   processing and aggregation of raw data files was performed with Affymetrix Power Tools

97   version 1.15.2, using apt-probe set-summarize and applying the robust multi-array

98   average algorithm. Sample quality control was performed using principal component

99   analysis as previously described (*6*).

100   *FGmRNA-profiling.* For a detailed description of FGmRNA-profiling we refer to

101   Fehrmann *et al.* (*4*). In short, we analyzed 77,840 expression profiles of publicly

102   available samples with principal component analysis and found that a limited number of

103   'Transcriptional Components' capture the major regulators of the mRNA transcriptome.

104   Subsequently, we identified a subset of 'Transcriptional Components' that described

105   non-genetic regulatory factors. We used these non-genetic Transcriptional Components

106   as covariates to correct microarray expression data and observed that the residual

107   expression signal (*i.e.* FGmRNA-profile) captures the downstream consequences of

108   genomic alterations on gene expression levels.

109   *Class comparison.* We performed a genome-wide class comparison analysis

110   (Welch's T-test) between FGmRNA-profiles of normal pancreatic tissue and PDA to

111   identify genes with upregulated FGmRNA-expression, which we considered a proxy for

112   protein expression. To correct for multiple testing, we performed this analysis within a

113   multivariate permutation test (1,000 permutations) with a false discovery rate of 1% and

114   a confidence level of 99%. This will result in a list of significant upregulated genes, which

115   contains (with a confidence level of 99%) no more than 1% false positives.

116   *Literature search on protein expression.* To compare targets identified with the class

117   comparison with known protein expression in PDA, we performed a literature search.

118   PubMed was searched for articles published in English from conception until February

119   2017. The following search terms were used: HUGO gene symbol of the target under

120   investigation in combination with '*pancreatic cancer*', '*expression*' and

121 *'immunohistochemistry'*. The cellular location and function of the protein product of the

122 gene was explored at http://www.genecards.org.

123

124 **Target Prioritization for Theranostic Approaches in PDA based on FGmRNA-**

125 **profiling**

126 The prioritization process consisted of 1) consulting the drug-gene interaction

127 database to select targets with a drug-gene interaction, 2) current status of (pre)clinical

128 evaluation of therapeutic drugs directed at the protein, 3) current status of (pre)clinical

129 evaluation of imaging tracers directed at the protein.

130 *Consulting the Drug-Gene Interaction Database (DGIdb) to identify drug-gene*

131 *interactions.* The DGIdb, accessible at dgibd.genome.wustl.edu, integrates data from 13

132 resources that includes disease-relevant human genes, drugs, drug-gene interactions

133 and potential druggability (*7*). Identified targets in the class comparison were explored in

134 the DGIdb to get insight into drug-gene interactions to enable selection of targets for

135 which a drug is available, or targets that are potential according to their membership in

136 gene categories associated with druggability.

137 *Current status of therapeutic efficacy at PubMed and Clinicaltrials.gov.* Targets for

138 which a drug-gene interaction was reported by the DGIdb were reviewed in literature to

139 determine the current status of drugs targeting these genes in clinical translation. 1) we

140 explored the efficacy of drugs targeting the protein in pancreatic cancer. 2) we explored

141 the efficacy of drugs targeting the protein in patients with other cancer types, because

142 these therapies might be relatively easily translated to pancreatic cancer patients 3) we

143 explored the knowledge in preclinical studies. PubMed was searched for articles

144 published in English from conception until February 2017 and clinicaltrials.gov was

145 explored for current (ongoing) clinical trials. PubMed was searched using the

146 combination of **1)** HUGO gene symbol of the target under investigation; '*pancreatic* AND

147 OR *cancer*'; and '*therapy*' or **2**) HUGO gene symbol*;* '*pancreatic* AND OR *cancer*'.

148   *Current status of evaluation of imaging targets at PubMed and Clinicaltrials.gov.* All

149 targets with a drug-gene interaction were reviewed in literature to prioritize targets that

150 are the furthest in clinical translation and have proved to be a suitable imaging target. An

151 additional PubMed search was executed for articles published in English form

152 conception until February 2017 to determine if the downstream proteins of these genes

153 are suitable as molecular imaging targets. We used the following search combinations:

154 'HUGO gene symbol'; '*pancreatic* AND OR *cancer*'; and '*imaging'*.

155

156 **RESULTS**

157 **FGmRNA-profiling: Identification of Upregulated Genes in PDA**

158   Supplemental Table 1 shows the datasets that were obtained from the Gene

159 Expression Omnibus. In total, 180 pancreatic samples were identified, which are derived

160 from 16 individual experiments; these samples consisted of 103 PDA and 77 normal

161 pancreatic samples. Class comparison analysis, with multivariate permutation testing

162 (false discovery rate 1%, confidence level 99%, 1 000 permutations), resulted in a set of

163 213 unique genes with significant FGmRNA-overexpression in PDA. Supplemental

164 Table 2 contains the class comparison for all genes.

165

166 **Literature Based Protein Expression Data for the Identified Top 50 targets**

167 **identified with FGmRNA-profiling**

168   Based on published immunohistochemistry results of the top 50 upregulated PDA

169   genes as described in Supplemental Table 3, 17/50 genes have a known downstream

170   protein overexpression in human PDA samples. The downstream protein

171   overexpression of 5/50 genes is described in other solid cancer types and therefore

172   these genes could be of interest for PDA. For 27/50 upregulated genes in PDA, no data

173   is available on protein expression in human cancers and therefore might be interesting

174   for preclinical validation in the near future.

175

176   **Prioritization of Potential Theranostic Targets in PDA**

177   Figure 1 shows the complete prioritization process. 94/213 upregulated genes in PDA

178   have a known drug-gene interaction according to DGIdb. Downstream proteins of 41/94

179   genes are currently investigated as a drug target for cancer treatment in clinical trials or

180   in preclinical studies (Fig. 2). 11/41 genes are investigated as antineoplastic drug targets

181   in clinical pancreatic cancer trials; 3/41 genes are investigated as antineoplastic drug

182   targets in clinical trials involving other solid cancer types, 12/41 genes are evaluated as

183   antineoplastic drug targets in preclinical *in vitro* and *in vivo* cancer-models and for 15/41

184   genes no antineoplastic drugs are currently available that target the downstream

185   proteins, but literature indicated involvement cancer development. Besides, downstream

186   proteins of 7/41 genes are currently described in the context of molecular imaging. We

187   are highlighting the studies evaluating the prioritized targets for molecular imaging

188   purposes in pancreatic cancer or in advanced clinical translation (Supplemental Table

189   4); a summary of the therapeutic studies can be found in Supplemental Table 5.

190   *Thymocyte differentiation antigen 1 (Thy1) – rank 1.* Molecular ultrasound imaging

191   using microbubbles targeting the membrane protein Thy1 detected tumors in transgenic

192 PDA mouse model with a diameter of only several millimeters in size could be visualized

193 with a 3-fold higher signal compared to normal pancreas tissue (*8*).

194   *CTSE – rank 8*. Ritonavir tetramethyl-BODIPY (RIT-TMB) is an optical imaging agent

195 based on a FDA-approved protease inhibitor. RIT-TMB showed CTSE specific imaging

196 in a PDA cell line (*9*). Another CTSE-activatable fluorescence imaging probe

197 demonstrated specific detection of CTSE activity in a PDA mouse model, in which the

198 fluorescence signal in the tumor was 3-fold higher than in background tissue (*10*).

199   *GGT5 – rank 10*. The cell membrane bound enzyme GGT5 can be targeted by

200 optical imaging probe γGlu-HMRG, which is only fluorescent after cleavage by GGT5

201 (*11*). γGlu-HMRG was topical applied on surgical breast cancer specimen to assess the

202 surgical margin. Tumors even smaller than 1 mm could be discriminated from normal

203 mammary gland tissue (*12*). In mouse models for colon cancer and disseminated

204 peritoneal ovarian cancer, tumors could be clearly visualized 1 min after topical

205 administration (*11,13*).

206   *MUC1 – rank 41*. The downstream cell membrane protein of *MUC1* is reported to be

207 overexpressed in 96% of the PDA cases. The [111]Indium labelled monoclonal antibody

208 PAM4 targeting MUC1 is suitable for single-photon emission tomography. In a clinical

209 phase I trial ^{111}In-PAM4 showed specific uptake of pancreatic cancer lesions (*14*). More

210 recently, the MUC1-specific optical imaging tracer Ab-FL-Cy5.5, which is a dual labelled

211 MUC1-targeting antibody conjugated to both a far-red dye and a green dye,

212 demonstrated specific uptake and *in vivo* visualization of ovarian cancer xenografts (*15*).

213 The MUC1 aptamer-based tracer APT-PEG-MPA showed that tracer uptake in the tumor

214 correlated well with MUC1 expression levels in MUC1-overexpressing hepatocellular

215 carcinoma and lung carcinoma cells in a xenograft mouse model (*16*).

216   *MSLN – rank 110.* The overexpression of the cell membrane protein MSLN has been

217   described in up to 86-100% of PDA cases (*17,18*). In a clinical phase I imaging trial, the

218   [89]zirconium labelled MSLN-antibody [89]Zr-MMOT0530A was administered in 11

219   metastatic cancer patients, seven with PDA and four with ovarian cancer. In all patients

220   at least one tumor lesion could be visualized (*19*). Beside this PET-tracer, a MSLN

221   specific tracer have been developed for single-photon emission tomography. [111]Indium

222   labelled amatuximab was investigated in six patients, of which two with PDA. In all

223   patients, at least one tumor lesion could be discriminated from its reference background

224   (*20*). Furthermore, the anti-MUC1 optical imaging tracer CT2, demonstrated selective

225   targeting of pancreatic cancer *in vitro* and in a pancreatic cancer orthotopic xenograft

226   model, tumors smaller than 5mm could be detected (*21*).

227

228   **DISCUSSION**

229   In this study, we were able to use FGmRNA-profiling on a substantial set of

230   normal pancreatic tissue and PDA tissue to predict protein overexpression for a large set

231   of targets and identified 213 upregulated targets in PDA, containing 41 currently

232   druggable targets with the potential for a theranostic approach in PDA patients.

233   Selection of suitable targets for imaging and/or therapy is complex. The ideal

234   target is highly overexpressed at the cell membrane of tumor cells and has a very limited

235   expression at the cell membrane of normal cells. Immunohistochemistry is a widely-used

236   method for the determination of protein expression at a cellular level. However, it is time

237   consuming and it demands many resources including access to formalin-fixed and

238   paraffin-embedded tissue samples of interest. Moreover, differences in execution of the

239   staining   protocol   and   scoring   methods   makes   it   difficult   to   compare

240 immunohistochemistry results from different studies. In contrary, FGmRNA profiling

241 enabled us to efficiently analyze and directly compare many genes as the predicted

242 overexpression is determined for each gene with the same methodology including a

243 large set of normal pancreatic tissue samples as a reference to determine the threshold

244 for 'overexpression'. Therefore, it has the advantage over immunohistochemistry for the

245 first selection of new therapeutical and imaging targets. FGmRNA-profiling previously

246 demonstrated it can guide clinicians and researches to select targets that needs further

247 preclinical validation, enabling a more efficient use of limited resources (*18,22*).

248   Theranostic drugs might be used for clinical decision making by enabling

249 visualization of molecular characteristics of the tumor to stratify patients for the most

250 optimal targeted therapy. Besides, theranostics can aid in monitoring treatment effects

251 helping clinicians to adjust therapy dose or to switch to another targeted drug. Based on

252 the current status of (pre)clinical evaluation of therapeutical drugs and imaging tracers

253 directed at downstream proteins of genes identified with FGmRNA-profiling, we

254 prioritized MUC1, MLSN, GGT5 and CTSE as current most potential theranostic targets.

255 These targets have already shown great potential to serve as a target for both therapy

256 and imaging in literature, indicating that these drugs have already made progress in the

257 clinical translation process and are potential for clinical translation in pancreatic cancer

258 patients on the short term. Other targets (*e.g.* THY1) first need to be validated as

259 suitable target, either therapeutical drugs and/or imaging tracers needs to be designed

260 and subsequently being investigated in preclinical studies before theranostic agents

261 targeting these proteins can be investigated in clinical trials.

262   Beside theranostic targets, FGmRNA-profiling can guide researchers and

263 clinicians in selecting targets for molecular imaging probes. After prioritization, only

264 seven out of the 41 currently druggable targets are described in the context of molecular

265 imaging, indicating the great potential of our results for development of favorable

266 molecular imaging probes. In PDA, molecular imaging might enhance disease staging

267 by enabling visualization of small PDA lesions, possibly leading to optimized selection of

268 patients that will benefit from curative surgery. Clinical trials already demonstrated the

269 feasibility of molecular fluorescence imaging in identifying micro metastases in

270 peritoneal metastasized ovarian- and colon cancer patients by targeting the folate alpha

271 receptor and vascular endothelial growth factor A (23-25). Besides, molecular imaging

272 can be used to better assess the extent of the primary tumor during PDA surgery and

273 evaluate essential resection planes. In PDA patients, two clinical trials are currently

274 registered that evaluate intraoperative molecular fluorescence imaging: targeting

275 vascular endothelial growth factor A (NCT02743975) and the epidermal growth factor

276 receptor (NCT02736578). FGmRNA-profiling predicted no overexpression of these

277 proteins which might negatively influence the likelihood of success compared to targets

278 highly rated by FGmRNA-profiling. However, beside alteration in gene expression levels,

279 mutation occurring in genes can result in different activation or functionality of the gene.

280 This phenomenon is not captured by FGmRNA-profiling, but could be relevant for certain

281 tumor phenotypes observed in PDA. For newly identified targets that are not highly rated

282 in the FGmRNA profiling we advise solid validation in *ex vivo* models and preclinical

283 models to confirm the validity of the target.

284 Furthermore, by fluorescently or radioactively labelling of therapeutic drugs,

285 molecular imaging can provide insight in pharmacokinetics, tumor uptake and

286 biodistribution which harbors the potential for drug development to select probes with

287 great therapeutic potential and to support optimal dosing and determine uptake in critical

288 organs to anticipate toxicity. This is especially relevant in PDA since a desmoplastic

289 reaction surrounding the tumor increases interstitial fluid pressure impairing drug

290 delivery. Therefore, molecular imaging might help to determine which probes might be

291 successfully translated into theranostic agents.

292   In conclusion, this study provides a data driven prioritization and overview of

293 imaging and therapeutic targets. The presented data can facilitate clinicians,

294 researchers and drug developers in deciding which therapeutical or imaging targets

295 should be taken for further clinical evaluation in PDA. This might help to improve disease

296 outcome of PDA patients in the short term.

Financial disclosure

302

303 **REFERENCES**

304 1. Siegel RL, Miller KD, Jemal A. Cancer Statistics, 2017. *CA Cancer J Clin*. 2017;67:7–30.

305 2. Oettle H, Neuhaus P, Hochhaus A, et al. Adjuvant chemotherapy with gemcitabine and
306 long-term outcomes among patients with resected pancreatic cancer: the CONKO-001
307 randomized trial. *JAMA*; 2013;310:1473–1481.

308 3. Conroy T, Desseigne F, Ychou M, et al. FOLFIRINOX versus gemcitabine for metastatic
309 pancreatic cancer. *N Engl J Med*. 2011;364:1817–1825.

310 4. Fehrmann RSN, Karjalainen JM, Krajewska M, et al. Gene expression analysis identifies
311 global gene dosage sensitivity in cancer. *Nat Genet.* 2015;47:115–25.

312 5. Barrett T, Wilhite SE, Ledoux P, et al. NCBI GEO: archive for functional genomics data
313 sets--update. *Nucleic Acids Res.* 2013;41:991–995.

314 6. Crijns APG, Fehrmann RSN, de Jong S, et al. Survival-related profile, pathways, and
315 transcription factors in ovarian cancer. *PLoS Med*. 3;6:e24.

316 7. Griffith M, Griffith OL, Coffman AC, et al. DGIdb: mining the druggable genome. *Nature*
317 *Methods.* 2013;10(12):1209–1210.

318 8. Foygel K, Wang H, Machtaler S, et al. Detection of pancreatic ductal adenocarcinoma in
319 mice by ultrasound imaging of thymocyte differentiation antigen 1. *Gastroenterology*.
320 2013;14:885–894

321 9. Keliher EJ, Reiner T, Earley S, et al. Targeting cathepsin E in pancreatic cancer by a
322 small molecule allows in vivo detection. *Neoplasia*. 2013;15:684–693.

323 10. Abd-Elgaliel WR, Cruz-Monserrate Z, Logsdon CD, Tung C-H. Molecular imaging of

14

324   Cathepsin E-positive tumors in mice using a novel protease-activatable fluorescent probe.

325   *Molecular BioSystems*. 2011;7:3207–3213.

326 11. Urano Y, Sakabe M, Kosaka N, et al. Rapid cancer detection by topically spraying a γ-

327   glutamyltranspeptidase-activated fluorescent probe. *Sci Transl Med*. 2011;3:110ra119.

328 12. Ueo H, Shinden Y, Tobo T, et al. Rapid intraoperative visualization of breast lesions with

329   γ-glutamyl hydroxymethyl rhodamine green. *Sci Rep*. 2015;5:12080.

330 13. Mitsunaga M, Kosaka N, Choyke PL, et al. Fluorescence endoscopic detection of murine

331   colitis-associated colon cancer by topically applied enzymatically rapid-activatable probe.

332   *Gut*. 2013;62:1179–1186.

333 14. Gold DV, Cardillo T, Goldenberg DM, Sharkey RM. Localization of pancreatic cancer with

334   radiolabeled monoclonal antibody PAM4. *Crit Rev Oncol Hematol*. 2001;39:147–154.

335 15. Zhang Q, Wang F, Wu Y-S, et al. Dual-color labeled anti-mucin 1 antibody for imaging of

336   ovarian cancer: A preliminary animal study. *Oncol Lett*. 2015;9:1231–1235.

337 16. Chen H, Zhao J, Zhang M, Yang H, Ma Y, Gu Y. MUC1 aptamer-based near-infrared

338   fluorescence probes for tumor imaging. *Mol Imaging Biol*. 2015;17:38–48.

339 17. Hassan R, Laszik ZG, Lerner M, Raffeld M, Postier R, Brackett D. Mesothelin is

340   overexpressed in pancreaticobiliary adenocarcinomas but not in normal pancreas and

341   chronic pancreatitis. *Am J Clin Pathol*. 2005;124:838–845.

342 19. Lamberts LE, de Groot DJA, Bense RD, de Vries EGE, Fehrmann RSN. Functional

343   genomic mRNA Profiling of a large cancer data base demonstrates mesothelin

344   overexpression in a broad range of tumor types. *Oncotarget*. 2015;6:28164-28172.

345 20. Lamberts L, Menke-van der Houven van Oordt CW, ter Weele EJ, et al.ImmunoPET with

346   Anti-Mesothelin Antibody in Patients with Pancreatic and Ovarian Cancer before Anti-

347   Mesothelin Antibody-Drug Conjugate Treatment. *Clin Cancer Res.* 2016;22:1642-1652

348 21. Lindenberg L, Thomas A, Adler S, et al. Safety and biodistribution of 111In-amatuximab in

349   patients with mesothelin expressing cancers using single photon emission computed

350   tomography-computed tomography (SPECT-CT) imaging. *Oncotarget.* 2015;6:4496–

351   4504.

352 22. Park JY, Hiroshima Y, Lee JY, Maawy AA, Hoffman RM, Bouvet M. MUC1 selectively

353   targets human pancreatic cancer in orthotopic nude mouse models. PLoS ONE.

354   2015;10:e0122100.

355 23. Hartmans E, Orian-Rousseau V, Matzke-Ogi A, et al. Functional genomic mrna profiling of

356   colorectal adenomas: identification and in vivovalidation of cd44 and splice variant cd44v6

357   as molecular imaging targets. *Theranostics.* 2017;7:482–492.

358 24. van Dam GM, Themelis G, Crane LMA, et al. Intraoperative tumor-specific fluorescence

359   imaging in ovarian cancer by folate receptor-α targeting: first in-human results. *Nat Med.*

360   2011;17:1315–1319.

361 25. Hoogstins CES, Tummers QRJG, Gaarenstroom KN, et al. A novel tumor-specific agent

362   for intraoperative near-infrared fluorescence imaging: a translational study in healthy

363   volunteers and patients with ovarian cancer. *Clinical Cancer Research.* 2016;22:2929–

364   2938.

365 26. Harlaar NJ, Koller M, de Jongh SJ, et al. Molecular fluorescence-guided surgery of

366   peritoneal carcinomatosis of colorectal origin: a single-centre feasibility study. *The Lancet*

367   *Gastroenterology & Hepatology.* 2016;1:283–290.

LEGENDS TO FIGURES
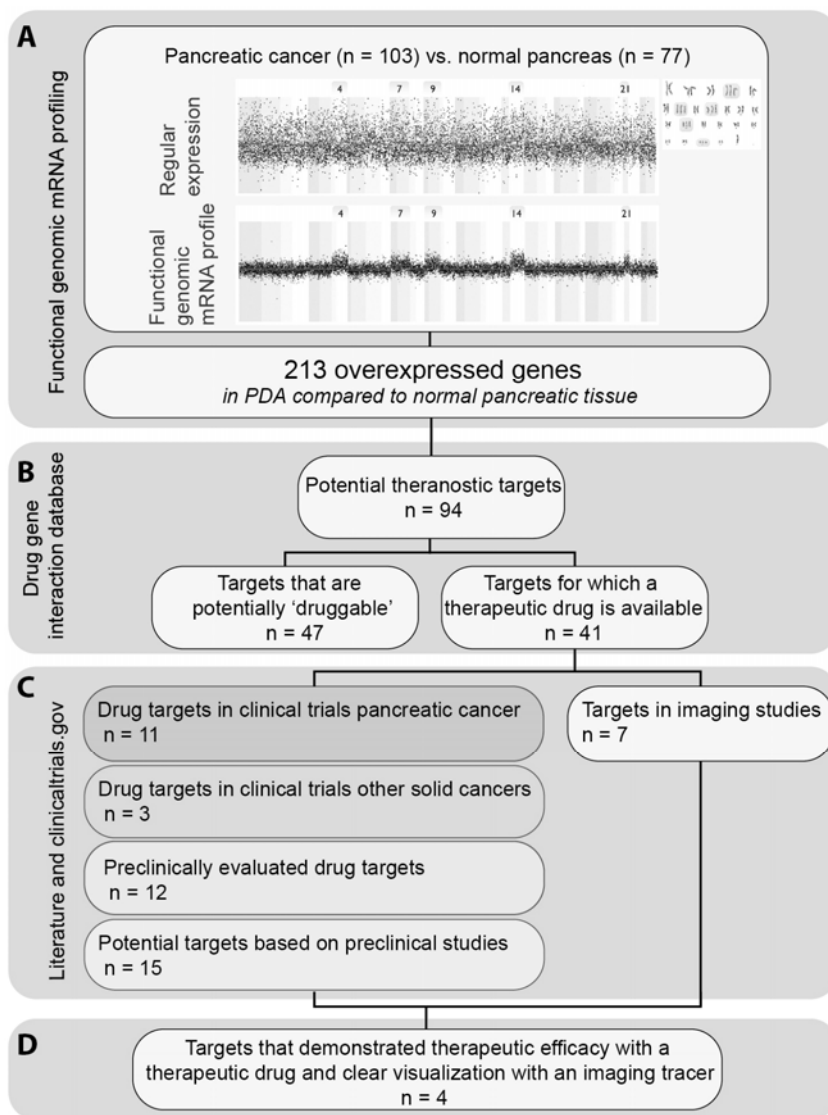
FIGURE 1 – The study flowchart shows the workflow for identification of current most potential targets for theranostic approaches in future PDA management. (A) We performed Functional genomic mRNA profiling to predict protein overexpression in PDA compared to normal pancreatic tissue. (B) Known interaction with antineoplastic drugs was explored at the Drug-Gene Interaction Database (DGIdB), and (C) we explored the current status of (pre)clinical evaluation of therapeutic and imaging strategies directed at the antigen. (D) we determined the most potential theranostic targets based on the

376   progress in clinical translation in both imaging and therapy to enable theranostic

377   approaches in PDA on short term. Abbreviations: PDA = pancreatic ductal

378   adenocarcinoma. FGmRNA = functional genomic mRNA.

379

380

381
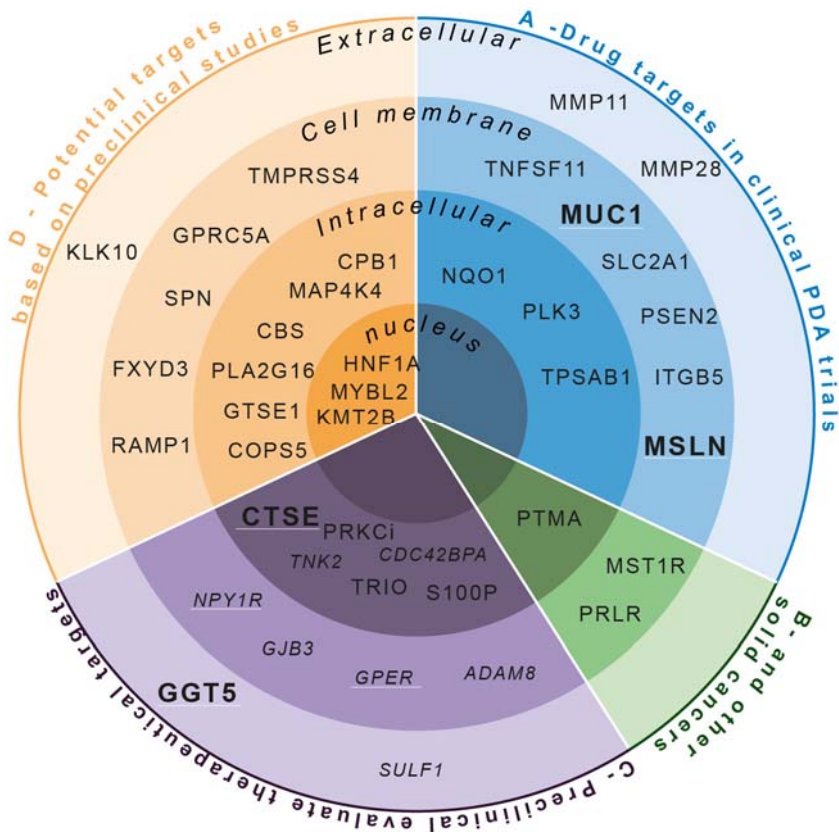
FIGURE 2 – The potential theranostic targets genes based on the Drug-Gene interaction database divided per cellular localization, per evaluation status. (A) Drug targets investigated in clinical trials in PDA patients. (B) Drug targets investigated in clinical trials in other cancer types. (C) Drug targets evaluated in preclinical studies. (D) Potential clinical targets that are currently not evaluated. In italic targets investigated *in vitro*. White underlined: targets evaluated in imaging studies. In bold: most potential theranostic targets.

Table 1. GEO omnibus datasets included in the study

profiling performed, year	GSE Accession number	normal pancreatic tissue	pancreatic cancer tissue
Walker et al (2004)	GSE1133	2	0
Buturovic et al (2008)	GSE12630	0	9
Badea et al (2009)	GSE15471	39	39
Sadanandam et al (2009)	GSE17891	0	1
Miya et al (2009)	GSE18674	1	0
Chelala et al (2009)	GSE19279	3	9
Hiraoka et al (2009)	GSE19650	7	0
Curley et al (2004)	GSE2109	0	16
Chen et al (2010)	GSE22780	8	0
Ge et al (2005)	GSE2361	1	0
Tran et al (2011)	GSE32676	7	25
Miya et al (2011)	GSE33846	1	0
Chelala et al (2013)	GSE43288	3	4
Kaneda et al (2013)	GSE43346	1	0
Blais et al (2013)	GSE46385	3	0
Roth et al (2007)	GSE7307	1	0

Abbreviation: GSE, gene expression omnibus series; PDA, pancreatic ductal adenocarcinoma

Note: GSE accession numbers can be used to query the data set in GEO (http://www.ncbi.nlm.nih.gov/geo/).

Supplemental Table 2 could not be added to PDF

Table 2. Literature overview protein overexpression human samples

Rank	Gene symbol	Protein location	Protein function	Protein overexpression in human samples			Reference
				PDA	other cancers	unkown	
1	THY1	cell membrane	Glycolipid	●			Foygel et al, 2013)
2	SEL1L	intracellular	unkown	●			Cattaneo et al, 2003
3	NPR3	Cell membrane	GPCR			●	
4	JUP /// KRT17	intracellular	cytokeratin		●		Escobar-Hoyos et al, 2014
5	NOX4	cell membrane	NADPH oxidase	●			Edderkaoui et al, 2005; Ogrunc et al, 2014
6	TM4SF1	cell membrane	Antigen	●			Lin et al, 2014
7	CLDN18	cell membrane	Tight junction protein	●			Tanaka et al, 2011; Wöll et al, 2014; Soini et al, 2012
8	CTSE	intracellular	Protease	●			Keliher et al, 2013
9	TMPRSS4	cell membrane	Protease	●			Wallrapp et al, 2000
10	GGT5	extracellular	Protease	●			Ramsay et al, 2014
11	DKK3	extracellular	unknown	●			Fong et al, 2009; Uchida et al, 2014
12	TINAGL1	extracellular	Glycoprotein			●	
13	LAMA3	extracellular	Laminin			●	
14	HSD17B7	cell membrane	SDR			●	
15	AHNAK2	intracellular	Unkown			●	
16	FXYD3	cell membrane	Ion channel regulator	●			Kayed et al, 2006
17	C7orf10	intracellular	Transferase			●	
18	GJB3	cell membrane	Gap junction protein			●	
19	GPRC5D	cell membrane	GPCR			●	
20	LAMC2	extracellular	Laminin	●			Garg et al, 2014; Katayama et al, 2005
21	MTMR11	intracellular	Phosphatase			●	
22	LRRC32	cell membrane	unknown			●	
23	HIST2H2AA3 /// HIS	intracellular	Nucleosome			●	
24	LIF	cell membrane	Growth factor	●			Peng et al, 2014
25	CST2	extracellular	Protease inhibitor			●	
26	CPB1	intracellular	Protease			●	
27	DCLRE1A	Intracellular	DNA repair gene			●	
28	ADAP1	intracellular	unkown			●	
29	PLA2G16	intracellular	Phospholipase		●		Nazarenko et al, 2006; Liang et al, 2015
30	MAP4K4	Intracellular	Kinase	●			Liang et al, 2008
31	HOPX *	nucleus	unknown				Waraya et al, 2012
32	ARL14	intracellular	Ribosylation Factor			●	
33	TP73-AS1	intracellular	Transcription factor			●	
34	CYP3A5	intacellular	Cytochrome p450			●	
35	TRIM29	intracellular	Transcription factor	●			Sun et al, 2014
36	DNAJB9	intracellular	J protein			●	
37	CAPRIN2	intracellular	unknown			●	
38	TRAK1	intracellular	Transporter		●		An et al, 2011
39	MRC1	cell membrane	Receptor			●	
40	LOC100653217 /// I	cell membrane	Cell adhesion molecule			●	
41	MUC1	cell membrane	Glycoprotein	●			Wang et al, 2014

No	Gene	Location	Function				Reference
42	*CBS*	intracellular	Lysase			●	
43	*UGT1A1 /// UGT1A*	intracellular	Transferase			●	
44	*GRB7*	cell membrane	Adaptor protein	●			Tanaka *et al*, 2006
45	*TREM2*	cell membrane	Receptor		●		Yang *et al*, 2014
46	*IGFBP5*	extracellular	growth factor binding protein	●			Johnson *et al*, 2006; Sarah K Johnson, 2009
47	*H2BFS*	intracellular	unknown			●	
48	*GSTM3*	intracellular	Transferase		●		Meding *et al*, 2012
49	*RTP4*	intracellular	Transporter			●	
50	*RUNX1T1*	intracellular	Transcription factor			●	

Abbreviation: GPRC, G-protein coupled receptor. SDR, Short Chain Dehydrogenase/Reductase

* Reduced protein expression level in cancer

Table 4 – Targets for pancreatic cancer imaging				
Tracer name	Study type	Cancer type	Conclusion	Reference
THY1, rank 1				
Thy1-Targeted Microbubbles (MBThy1)	in vivo - *mouse ultrasound molecular imaging*	pancreatic cancer xenofgrafts	Thy1 targeted ultrasound molecular imaging is feasible	Foygel *et al*, 2013
CTSE, rank 8				
CTSE-activatable optical molecular probe	in vivo - *mouse optical imaging*	pancreatic cancer xenofgrafts	CTSE-activatable probe can be detected by confocal laser endomicroscopy (CLE)	Li *et al*, 2014
ritonavir tetramethyl-BODIPY (RIT-TMB)	in vivo - *mouse optical imaging*	pancreatic cancer orthotopic tumors	RIT-TMB imaging is feasible *in vitro* and demonstrated good co- localization with CTSE in both humand and mouse PDA samples	Keliher *et al*, 2013
CTSE-activatable optical molecular probe	in vivo - *mouse optical imaging*	pancreatic cancer xenofgrafts	The Cath E-activatable probe was able to highlight the Cath E-positive tumors; control imaging probe confirmed the superior selectivity and sensitivity	Abd-Elgaliel *et al*, 2011
GGT5, rank 10				
gGlu-HMRG	*ex vivo optical imaging EUS-FNA*	Human pancreatic samples	gGlu-HMRG did not clearly differentiate pancreatic tumor tissues from normal pancreatic ones because GGT activity was not different between tumor cells and normal cells.	
gGlu-HMRG	ex vivo breast cancer samples	Breast cancer	fluorescence derived from cleavage of gGlu-HMRG allowed easy discrimination of breast tumors from normal mammary gland tissues, with 92% sensitivity and 94% specificity.	Ueo *et al*, 2015
BODIPY-GSH	*In vitro*	Ovarian cancer cells	FIST probes enable monitoring the GGT activity in living cells,which showed differentiation between ovarian cancer cells and normal cells.	Wang *et al*, 2015
gGlu-HMRG	*Ex vivo*	colon carcinoma samples	Topically spraying gGlu-HMRG enabled rapid and selective fluorescent imaging of colorectal tumors owing to the upregulated GGT activity in cancer cells.	Sato *et al*, 2015
gGlu-HMRG	*In vivo - mouse*	Colon cancer mouse model	Fluorescence endoscopic detection of colon cancer was feasible. All fluorescent lesions contained cancer or high-grade dysplasia, all non-fluorescent lesions contained low-grade dysplasia or benign tissue.	Mitsunaga *et al*, 2013
gGlu-HMRG	*In vivo - mouse*	disseminated peritoneal ovarian cancer model	Activation of gGlu-HMRG occurred within 1 min of topically spraying the tumor, creating high signal contrast between the tumor and the background.	Urano *et al*, 2011
MUC1, rank 41				
aptamer-PEG-near- infrared fluorescence probe (APT-PEG-MPA)	*in vivo - mouse optical imaging*	breast cancer, non-small cell lung carcinoma, hepatocellular carcinoma xenografts	MUC1 aptamer-based NIR fluorescence probe has a high tumor-targetinga ability and low accumulation in normal tissue	Chen *et al*, 2015
MN-EPPT (iron oxide nanoparticles (MN), labeled with Cy5.5 dye conjugated to peptides (EPPT)	in vivo - *mouse optical imaging/MRI*	breast cancer transgenic mouse model	changes in uMUC-1 expression during tumor development and therapeutic intervention could be monitored non-invasively using molecular imaging approach with the uMUC-1-specific contrast agent (MN-EPPT) detectable by magnetic resonance and fluorescence optical imaging	Ghosh *et al*, 2013

(111)In-labeled PAM4	*phase I clinical trial* <u>PET-scan</u>	pancreatic cancer	radiolabeled PAM4 selectively targets pancreatic cancer in both the experimental animal model and clinical studies.	Gold *et al*, 2001
[64Cu]-DOTA-PR81	*in vivo - mouse* <u>PET-scan</u>	breast cancer xenografts	The biodistribution and scintigraphy studies showed the accumulation of 64Cu-DOTA-PR81 at the site of tumors with high sensitivity and specificity for MUC1 compared to control probes.	Alirezapour *et al*, 2016
Ab-FL-Cy5.5	*in vivo - mouse* <u>*dual labelled optical imaging*</u>	ovarian cancer xenografts	Ab-FL-Cy5.5 probe can be used for *in vivo* imaging of MUC1 expressing tumors	Zhang *et al*, 2015
NPY1R, rank 92				
[Lys(M/DOTA)4] BVD15	*in vitro*	Breast cancer cells	[Lys(DOTA)4]BVD15 is a potent and specific ligand for NPY1R	Zhang *et al*, 2016
MSLN, rank 110				
89Zr-MMOT0530A+E36:I4089Zr-MMOT0530A	*phase I clinical trial* <u>PET-scan</u>	pancreatic cancer and ovarian cancer	89Zr-MMOT0530A-PET pancreatic and ovarian cancer lesions as well as antibody biodistribution could be visualized.	Lamberts *et al*, 2015b
64Cu-NOTA-amatuximab	in vivo - *mouse* <u>*PET-scan*</u>	epithelial carcinoma cells	64Cu-NOTA-amatuximab enables quantification of tumor and major organ uptake values using PET scanning	Lee *et al*, 2015
Indium-CHX-A amatuximab	*phase I clinical trial* <u>SPECT-scan</u>	mesothelin overexpressing tumors	111In-amatuximab localizes to mesothelin expressing cancers with a higher uptake in mesothelioma than pancreatic cancer.	NCT01521325
Me-F127COOH-QD nanomicelles	*in vivo - mouse*	pancreatic cancer xenofgrafts	anti-mesothein antibody conjugated carboxylated F127 nanomicelles accumulated specifically at the pancreatic tumor site 15 min after intravenous injection with low toxicity	Ding *et al*, 2011
anti-mesothelin antibody-conjugated PEGlyated liposomal ultrasmall superparamagnetic iron oxides	*in vivo - mouse* <u>*MRI*</u>	pancreatic cancer xenofgrafts	M-PLDUs specically targets MSLN and could well improve the therapeutic efficacy of DOX chemotherapy in vivo and could be visualized by MRI in vivo.	Deng *et al*, 2012
GPER, rank 118				
99mTc(I)-labeled nonsteroidal GPER-specific ligands	in vivo - *mouse* SPECT-scan	human endometrial and breast cancer cell xenografts	99mTc-labeled-GPER-specific radioligands are tumor specific and could be cleary visualized using SPECT-scan	Nayak *et al*, 2014

Supplementary table 3. Therapeutical targets for pancreatic cancer treatment					
Antineoplastic drug	Therapy type	Study population	Phase	Conclusion / status study	Reference / clinicaltrial.gov identifier
Subcategory 1. Targets in pancreatic cancer clinical trials					
MUC1, rank 41					
MUC1 100mer peptide with SB-AS2 adjuvant	cancer vaccine	unresectable PDA	I	feasible	Ramanathan *et al*, 2005; NCT00008099
MUC1 100mer peptide	cancer vaccine	unresectable PDA	I	1/6 SD	Yamamoto *et al*, 2005
MUC1-DC and MUC1-CTL	adoptive immunotherapy	unresectable PDA	I	1/20 CR 5/20 SD	Kondo *et al*, 2008
MUC1-DC	adoptive immunotherapy	Advanced PDA	I	7/7 PD	Rong *et al*, 2012
90Y-hPAM4	radio-immunotherapy	Advanced PDA	I/II	6/38 PR 16/38 SD	Ocean *et al*, 2012; NCT00603863
Falimarev (fowlpox-CEA-MUC-1-TRICOM vaccine) Inalimarev (vaccinia-CEA-MUC1-TRICOM vaccine)	cancer vaccine	unresectable PDA	I	recruiting	NCT00669734
anti-MUC1 CAR T Cells	immunotherapy	advanced, refractory solid tumors	I/II	recruiting	NCT02587689
anti-MUC1 CAR-pNK cells	immunotherapy	Relapsed or Refractory Solid Tumor	I/II	rectruiting	NCT02839954
NQO1, rank 53					
Apaziquone	bioreductive prodrug activated by NQO1	Pancreatic cancer first line	II	Antitumour activity was not observed.	Dirix *et al*, 1996
PSEN2, rank 54					
MK-0752	NOTCH inhibitor	unresectable PDA	I	completed no results yet	NCT01098344
TNFSF11, rank 57					
Lenalidomide	immunotherapy	metastatic PDA	II	PR: 8/72 SD: 26/72 PD: 22/72 MOS 4.7 months	Infante *et al*, 2013
ITGB5, rank 65					
Cilengitide	anti-angiogenic therapy	unresectable PDA	II	C+G MOS: 6.7 months gemcitabine MOS: 7.7 months	Friess *et al*, 2006
MSLN, rank 110					
BAY94-9343	antibody drug conjugate	advanced, refractory solid tumors	I	recruiting	NCT02485119
BMS-986148	antibody drug conjugate	mesothelin positive pancreatic cancer	I	recruiting	NCT02341625
CART-meso	immunotoxin	metastatic mesothelin expressing cancers	I/II	recruiting	NCT01583686

CART-meso	immunotoxin	Mesothelin expressing cancers	I	recruiting	NCT02159716
CART-meso	immunotoxin	metastatic PDA	I	recruiting	NCT02465983
CART-meso	immunotoxin	metastatic PDA	I	safe and feasible	Beatty *et al*, 2014
CART-meso	immunotoxin	Metastatic	I/II	recruiting	NCT02959151
CART-meso	immunotoxin	PDA			
CART-meso	immunotoxin	PDA	I	recruiting	NCT02706782
SS1P(dsFv)-PE38	immunotoxin	unresectable or metastatic PDA	I/II	recruiting	NCT01362790
SS1P(dsFv)-PE39	immunotoxin	Mesothelin expressing cancers	I	SS1p is well tolerated	Hassan *et al*, 2007
SS1P(dsFv)-PE40	immunotoxin	mesothelin experessing cancers	I	SS1p is well tolerated	Kreitman *et al*, 2009
Morab-009 (amatuximab)	antibody	mesothelin expressing cancers	I	safe and feasible	Hassan *et al*, 2010
Morab-009 (amatuximab)	antibody	unresectable PDA	II	completed, no article published yet	NCT00570713
GVAX (GM-CSF)	immunotherapy	Advanced PDA	I	safe and feasible	Laheru *et al*, 2008
GVAX (GM-CSF)	immunotherapy	PDA, adjuvant;	II	PD: 17/60 MOS: 24.8 months	Lutz *et al*, 2011
ANZ-100 and CRS-207	cancer vaccine	metastatic PDA	I	Safe and feasible OS: 3/7 > 15months	Le *et al*, 2012
GVAX and CRS-207	cancer vaccine	metastatic PDA	II	cy/GVAX and CRS-207: OS 9.7 months cy/GVAX: OS 4.6 months	Le *et al*, 2015
LMB-100 + Nab-Paclitaxel	Immunotoxin combined with chemotherapy	Pancreatic Neoplasms	I/II	recruiting	NCT02810418
Anetumab ravtansine	Antibody drug conjugate	Pretreated Advanced Pancreatic Cancer	II	not yet recruiting	NCT03023722
SLC2A1, rank 154					
Glufosfamide vs F-5U	chemotherapy	metastatic PDA	III	recruiting	NCT01954992
Glufosfamide	chemotherapy	Advanced PDA	II	PR: 2/34 SD: 11/35 MOS: 5.3 months	Briasoulis *et al*, 2003
Glufosfamide + gemcitabine	chemotherapy	metastatic PDA	II	PR: 5/28 SD: 11/28 MOS: 6 months	Chiorean *et al*, 2010
Glufosfamide vs best supportive care	chemotherapy	metastatic PDA	III	MOS glufosfamide: 105 days MOS best supportive care: 84 days	Ciuleanu *et al*, 2009

PLK3, rank 148					
BI 2536	Polo-like kinase inhibitor	unresectable advanced PDA	II	PR: 2/79 SD: 19/79 MOS: 149 days	Mross *et al*, 2012
TPSAB1, rank 184					
nafamostat + gemcitabine	protease inhibitor + chemotherapy	advanced or metastatic PDA	I	PR: 3/12 SD: 7/12 PD: 2/7	Uwagawa *et al*, 2009
nafamostat + gemcitabine	protease inhibitor + chemotherapy	unresectable advanced or metastatic PDA	II	PR: 6/35 SD: 25/34 PD: 4/35 MOS: 10 months	Uwagawa *et al*, 2013
MMP11, rank 166					
marimastat vs gemcitabine	MMP inhibitor + chemotherapy	unresectable advanced or metastatic PDA	III	MOS gemcitabine: 167 days MOS 25mg: 125 days MOS 10mg: 105 days MOS 5 mg: 110 days	Bramhall *et al*, 2001
MMP28, rank 199					
marimastat	MMP inhibitor	Advanced PDA	II	SD: 41/83 in 28 day study period PD: 42/83 in 28 day study period MOS: 113 days	Bramhall *et al*, 2002
Subcategory 2. Targets in clinical trials in other cancer types					
MST1R, rank 95					
Foretinib	small-molecule multikinase inhibitor	advanced or metastatic gastric adenocarcinoma	II	PR: 0/69 SD: 15/65 lack of efficacy	Shah *et al*, 2013
Foretinib	small-molecule multikinase inhibitor	papillary renal cell carcinoma	II	ORR: 13.5% MPFS: 9.3 month	Choueiri *et al*, 2013
MGCD265	Tyrosine kinase inhibitor	Advanced metastatic or unresectable malignancy	I	recruiting	NCT00697632
MGCD266	Tyrosine kinase inhibitor	advanced or metastatic non-small cell lung cancer	II	recruiting	NCT02544633
PTMA, rank 106					
Thymalfasin / Thymosin 1 / (T-alfa-1)	Immunomodulatory polypeptide	metastatic esophageal cancer	II	not yet recruiting	NCT02545751
Thymalfasin / Thymosin 1 / (T-alfa-1)	Immunomodulatory polypeptide	metastatic small cell lung cancer	II	not yet recruiting	NCT02542137

Thymalfasin / Thymosin 1 / (T-alfa-1)	Immunomodulatory polypeptide	metastatic non small cell lung cancer	II	not yet recruiting	NCT02542930
Thymalfasin / Thymosin 1 / (T-alfa-1)	Immunomodulatory polypeptide	metastatic colon cancer	II	not yet recruiting	NCT02535988
Thymalfasin / Thymosin 1 / (T-alfa-1)	Immunomodulatory polypeptide	hepatocellular carcinoma	IV	not yet recruiting	NCT02281266
Thymalfasin / Thymosin 1 / (T-alfa-1)	Immunomodulatory polypeptide	metastatic melanoma patients	I	MOS: 9.4 months vs. 6.6 months	Maio *et al*, 2010
PRLR, rank 213					
prolanta	prolactine receptor antagonist	Epithelial ovarian cancer	I	recruiting	NCT02534922
LFA102	monoclonal antibody	breast and prostate cancer	I	completed, no results published	NCT01338831
Subcategory 3. Targets in preclinical *in vitro* and *in vivo* studies					
CTSE, rank 8					
Cathepsin E-activatable 5-ALA prodrug	photo dynamic therapy	in vivo - mouse PDA cells		Effectively targeting and killing cancer cells that express CTSE	Abd-Elgaliel *et al*, 2013
GGT5, rank 10					
GSAO (glutathione-S-conjugate activated by γGT cleavage)	prodrug	in vivo - PDA mouse model		Tumor γGT activity positively correlated with GSAO-mediated inhibition of pancreatic tumor angiogenesis and tumor growth in mice.	Ramsay *et al*, 2014
GJB3, rank 18					
Carbenoxolone	gap junction blocker	in vitro - Pancreatic stellate cells		Carbenoxolone inhibited platelet-derived growth factor-BB-induced proliferation and migration	Masamune *et al*, 2013
TNK2, rank 73					

AIM-100 pyrazolopyrimidine derivative 2b ALK inhibitor 5	TNK2 inhibitors	in vitro - prostate cancer cells		AIM-100 treatment is leading to cell cycle arrest in the G1 phase causing significant decrease in the proliferation of pancreatic cancer cells and induction of apoptosis.	Mahajan *et al*, 2012
(*R*)-9bMS	small-molecule inhibitor	triple negative breast cancer (TNBC)		In vitro inhibition significantly compromised TNBC proliferation	Wu et al, 2017
NPY1R, rank 92					
BIBP3226	peptide-drug conjugate	in vitro - neuroblastoma cells		The active compund BIBP3226 is able to release the drug intracellular	Langer *et al*, 2001
TRIO, rank 107					
TRIP-E32G	peptide aptamer	In vivo - NIH 3T3 cells		TRIPE32G reduces the formation of TRIO-induced tumors.	Bouquier *et al*, 2009
GPER, rank 118					
Gefitinib	Tyrosine Kinase inhibitor	In vitro – Triple-negative breast cancers cells		Reduction of GPER expression is a promising therapeutic approach for TNBC	Girgert *et al*, 2017

agonist G-1	GPER-receptor-agonist	In vitro – nonsmall cell lung cancer cells		G-1 treatment rapidly decreased the phosphorylation, nuclear translocation, and promoter activities of NF-κB, which will help to better understand the roles and mechanisms of GPER as a potential therapy target	Zhu *et al*, 2016
ADAM18, rank 141					
BK-1361	ADAM8 inhibitor	in vitro - PDA cells		BK-1361 decreased tumour burden and metastasis of implanted pancreatic tumour cells in mice	Schlomann *et al*, 2015
CDC42BPA, rank 142					
DJ4	small molecule inhibitor	in vitro - (PDA) cells		DJ4 treatment significantly blocked stress fiber formation and inhibited migration and invasion of multiple cancer cell lines	Kale *et al*, 2014
PRKCi, rank 161					
aPKC-PSP	pseudosubstrate peptide	In vivo -glioblastoma Stem-like cells (GSC)		Targeting PKCι in the context of Notch signaling could be an effective way of attacking the GSC population in GBM	Phillips *et al*, 2016
SULF1, rank 180					

				Quinazolinone-based radiopharmaceuticals can lead to the development of a novel noninvasive approach for imaging and treating pancreatic cancer.	
IQ2-S	radioactive prodrug	in vitro - PDA cells			Pospisil *et al*, 2012

S100P, rank 188

				C5OH blocked the S100P-mediated growth and antiapoptotic effect in PDA and improved the animal survival.	
cromolyn	cromolyn analog, C5OH	in vivo - PDA mouse			Arumugam *et al*, 2013
2H8	S100P antibody	in vivo - mouse - PxPC3 cells		2H8 antibody decreased tumor growth and liver metastasis formation in a subcutaneous and orthotopic BxPC3 tumor model.	Dakhel *et al*, 2014

Subcategory 4. Suggested as potential targets

	Cancer type	Study type		Conclusion stu	Reference
TMPRSS4, rank 9					
	breast cancer tissue	IHC		Prognostic marker	Liang *et al*, 2013
	Non-small cell lung cancer (NSCLC)	In vitro treatment with demethylating agent significantly increased TMPRSS4 levels		Potential therapeutic target	Villalba *et al*, 2016
	Gastric cancer	Upregulation of TMPRSS4 enhances the invasiveness of gastric cancer cells		Potential therapeutic target	Jin *et al*, 2016
FXYD3, rank 16					

	Breast cancer	Suppression of FXYD3 by transfection with siRNA		Overexpression of FXYD3 may be a marker of resistance to cancer treatments and a potentially important therapeutic target.	Liu *et al*, 2016a

CPB1, rank 26

	Metastasis in Low Grade Breast Cancer samples	IHC		Biomarker	Bouchal *et al*, 2015

PLA2G16, rank 29

	Osteosarcoma	In vitro and in vivo functional analyses		Potential therapeutic target	Li *et al*, 2016

MAP4K4, rank 30

	Gastric cancer	In vitro siilencing of MAP4K4 by shRNA		Potential therapeutic strategy	Liu *et al*, 2016b

CBS, rank 42

	in vitro - mouse	CBS silencing		CBS silencing resulted in reduced tumor cells proliferation, blood vessels formation and lipid content.	Chakraborty *et al*, 2015
	Colon cancer	In vivo - xenograft		Benserazide inhibits CBS activity and suppresses colon cancer cell proliferation and bioenergetics in vitro, and tumor growth in vivo	Druzhyna *et al*, 2016

GPRC5A, rank 70

	colon cancer samples	IHC		Prognostic biomarker	Zougman *et al*, 2013
	oral squamous cell carcinoma	IHC		Prognostic biomarker	Liu *et al*, 2013
	gastric cancer samples	mRNA expression levels		Prognostic biomarker	Liu *et al*, 2015

	PDAC cells	siRNA		Suppression of GPRC5a results in decreased cell growth, proliferation and migration	Jahny *et al*, 2017
	breast cancer cell line	siRNA		Transfection of siRNA suppressed RAI3 mRNA and growth of the cancer cells.	Nagahata *et al*, 2005

KLK10, rank 79

	Breast cancer	RNA-Sequencing analysis		Predictive biomarker for trastuzumab resistance and potential therapeutic target for reversing trastuzumab resistance	Wang *et al*, 2016

COPS5, rank 93

	Breast cancer	Integrated genomic and functional studies		COPS5 overexpression causes tamoxifen-resistance in preclinical breast cancer models in vitro and in vivo > potential therapeutic approach for endocrine-resistant breast cancer	Lu *et al*, 2016

GTSE1, rank 97

	Gastric cancer cells	shRNA GTSE1 knockout		Biomarker. Potential therapeutical target.	Deeb *et al*, 2014

hepatocellular carcinoma cells	shRNA GTSE1 silencing		GTSE1 is aberrantly overexpressed in HCC cell lines and cancerous tissues > Potential therapeutic target	Guo *et al*, 2016

KMT2B, rank 104

Breast cancer cell	siRNA knockdown		Inhibition of IL-20 and KMT2B may have therapeutic benefits in ERα-positive breast cancer	Su *et al*, 2016

SPN, rank 160

HPB-ALL lymphol	UN1 monoclonal antibody		UN1 mAb is leading to natural killer–mediated cytotoxicity causing growth inhibition	Tuccillo *et al*, 2014
mouse model - br	siRNA SPN knockdown		Reduction in primary tumour growth in vivo	Fu *et al*, 2014

RAMP1, rank 166

prostate cancer			Potential molecular target	Logan *et al*, 2013

HNF1A, rank 167

PDA tissue and cells	siRNA HNF1A knockdown		siRNA HNF1A knockdown reduced apoptosis in pancreatic cancer cell lines. HNF1A is a possible tumor suppressor	Luo *et al*, 2015

MYBL2, rank 181

In vivo - mouse Breast cancer xenografts	Si-RNA		B-myb plays a role in cell cycle progression and tumorigenesis. Potential diagnostic / therapeutical target	Tao *et al*, 2014